European Conference on Optical Communication (ECOC) 2022 ©
Optica Publishing Group 2022

Class-80 InP-based high-bandwidth coherent driver modulator with flexible printed circuit RF interface

Josuke Ozaki [(1)], Yoshihiro Ogiso[(1)], Yasuaki Hashizume[(1)], Hiroshi Yamazaki[(2)], Kazuya Nagashima[(3)], Mitsuteru Ishikawa[(1)]

[(1)] NTT Device Innovation Center, NTT Corporation, 3-1 Morinosato Wakamiya, Atsugi, Kanagawa, 243-0198, Japan, josuke.ozaki.mp@hco.ntt.co.jp
[(2)] NTT Device Technology Labs, NTT Corporation, 3-1 Morinosato Wakamiya, Atsugi, Kanagawa, 243-0198, Japan
[(3)] Telecommunications & Energy Laboratories, Furukawa Electric Co., Ltd., 6 Yawata-kaigandori, Ichihara, Chiba, 290-8555, Japan

Abstract *We developed flexible printed circuit RF interface InP-based coherent driver modulators with a 3-dB bandwidth of over 80 GHz for 128-Gbaud or higher operations. Low insertion loss (<8.5 dB per polarization), low polarization-dependent loss (<0.1 dB), and high extinction ratio (>30 dB) were achieved.*

Introduction

High capacity optical transport networks are required to meet the demand of increasing global IP traffic. Higher baud-rate and higher-order optical quadrature amplitude modulation (QAM) are key to enhancing the capacity of digital coherent optical systems [1,2]. A high-bandwidth coherent driver modulator (HB-CDM) [3,4] and high-bandwidth intradyne coherent receiver (HB-ICR) [5,6] are important devices for high-speed transmission systems. In the HB-CDM configuration, a driver IC and a dual-polarization (DP) IQ modulator are assembled adjacent to each other in one package to reduce the radio-frequency (RF) loss and footprint. Standardization of the HB-CDM supporting operations at up to 128 Gbaud has been completed at the Optical Internetworking Forum (OIF) [4]. The HB-CDM for 128-Gbaud operations called class-80. The class number refers to the approximate EO 3-dB bandwidth. The highest 3-dB bandwidth of HB-CDM reported so far is 66.7 GHz [7], but there are no reports of HB-CDMs with 3-dB bandwidth over 80 GHz (class-80) yet.

Regarding a modulator photonic integrated circuit (PIC) for the HB-CDM, InP-based Mach-Zehnder modulators have been widely used because of their advantages of small size, low driving voltage and high bandwidth. Recently, a small thin-film $LiNbO_3$ (LN) modulator with low half-wavelength voltage (V_π) and high bandwidth has been reported [8]. Furthermore, a HB-CDM using a thin-film LN modulator has been presented [9]. From the view point of efficient connection with a driver IC, a modulator with differential drive is preferable to maximize the performance of the driver. However, the thin-film LN modulators reported so far are not differential drive but single-ended drive [10].

As for HB-CDM RF packages, the HB-CDMs reported so far use a package with a surface-mount-type (SMT) RF interface. However, the SMT packages have a roll-off frequency below 70 GHz [11] due to the lead pin structure, the connection configuration between the printed circuit board (PCB) and lead pins, and the usage of RF vias. Therefore, the RF characteristics of the SMT package are insufficient to achieve a class-80 HB-CDM.

In this paper, we report the first class-80 HB-CDM with a flexible printed circuit (FPC) RF interface to break through the bandwidth limitation imposed by the SMT package. This HB-CDM integrates a high-speed and low-propagation-loss InP-based n-i-p-n heterostructure modulator PIC with a differential capacitively loaded traveling-wave electrode (CL-TWE) [12] and a 4-channel linear SiGe BiCMOS driver IC with an open-collector configuration. By using these components, an electro-optic (EO) 3-dB bandwidth of over 80 GHz was achieved for the first time by using the HB-CDM configuration. In addition, important optical characteristics were excellent, such as an insertion loss (IL) <8.5 dB per polarization, polarization-dependent loss (PDL) <0.1 dB, and extinction ratio (ER) >30 dB.

Design

Figure 1 shows a photograph of the developed class-80 HB-CDM. The package body measures 12 x 30 x 5.3 mm^3. The RF and DC interfaces of

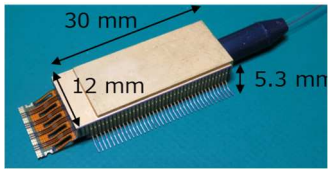

Fig. 1: Photograph of fabricated HB-CDM.

the package are based on an FPC and SMT, respectively. To improve the RF characteristics, the FPC is used as the RF interface, and the SMT is used as the DC interface for compatibility with conventional HB-CDMs. The FPC is made of polyimide and the RF trace length on the FPC is less than 10 mm. The SiGe BiCMOS 4-ch driver and the InP-based n-i-p-n heterostructure modulator PIC mounted on a thermoelectric cooler (TEC) are assembled in the package.

Figure 2 shows simulation results comparing the RF characteristics (S_{dd21}) of the package with the SMT RF interface and FPC RF interface. The FPC package simulation model had a channel pitch of 2.4 mm, the signal-to-signal pad pitch of 0.45 mm, the PCB length (from the FPC connection) of 2.5 mm, and the FPC length of 15 mm. The same channel pitch and PCB length were used for the SMT model, and the two different signal-to-signal lead pitches (0.8 mm and 0.65 mm) were simulated. The results confirmed that the roll-off frequency can be improved by narrowing the signal-to-signal pitch (0.8 mm to 0.65 mm). However, it is difficult to further reduce the pitch from the viewpoint of assembly. The SMT package has a roll-off frequency at frequencies below 80 GHz, which is not sufficient for a class-80 HB-CDM package. On the other hand, the roll-off frequency is over 90 GHz for the FPC package which is sufficient for class 80 or higher.

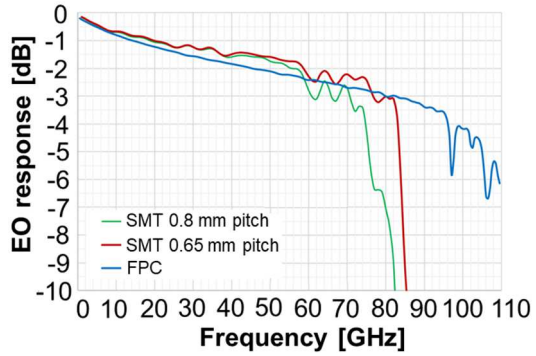

Fig. 2: RF simulation results (S_{dd21}) of SMT package and FPC package.

Next, the design and characteristics of the modulator PIC and driver are described. Since there is a trade-off between the modulator bandwidth and the characteristic impedance, the impedance is designed to be 60 Ω based on the idea of coordinated design with the driver. In this design, the EO 3-dB bandwidth of the modulator PIC is more than 60 GHz, and V_π is below 2 V. The modulator PIC integrates an SSC with little process variation to stabilize the optical mode field and the lens coupling loss. A heater is employed as a phase controller. By using the heater and eliminating the active region by regrowth except for the RF section, the propagation loss is reduced compared to a phase-adjusted electrode using the EO effect. Furthermore, the n-i-p-n structure is more effective at reducing optical and RF losses compared with the conventional p-i-n structure because the thickness of the p-layer, which has a significant impact on the optical and RF losses, is thinner. These techniques have led to very good optical propagation loss, equivalent to or lower than that of conventional LN modulators. A SiGe BiCMOS 4-channel linear differential open-collector driver with an amplitude of 2.5 Vppd and a 3-dB electrical bandwidth of over 90 GHz is used. In addition, for efficient connection of the driver and modulator, it is important to reduce the connection inductance between the driver and modulator. In this HB-CDM, double wires are used and the gap between the modulator and driver is kept to less than 30 um, resulting in an inductance of about 70 pH.

Experimental Results

Figure 3 shows the EO response of the fabricated CDM. The HB-CDM was soldered to an evaluation board and the board's RF loss of the transmission line and G3PO connector after 2.5 mm from the FPC edge on the board was de-embedded by using a test coupon. A 3-dB EO bandwidth of over 80 GHz was confirmed. To the best of our knowledge, this is the highest EO bandwidth ever reported for HB-CDMs.

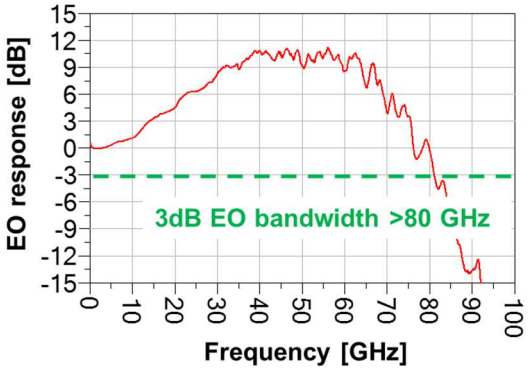

Fig. 3: EO response of the HB-CDM

Figure 4 and 5 shows the IL per polarization at the maximum transmission and the ER of the HB-CDM over the C-band. The low loss of the modulator PIC and the mode field stabilization of the input/output waveguide, which suppress the lens coupling loss, have resulted in a very low IL of <8.5 dB and PDL of <0.1 dB. The optical propagation loss per polarization at the maximum transmission in the modulator chip is less than 6.0 dB over the C-band and the coupling loss between the modulator PIC and input/output fibers (including optical component loss) is about

2.5 dB. By taking care of the generation of the higher-order modes in the chip, we achieved an ER of more than 30 dB over the C-band of the child Mach-Zehnder interferometer of the modulator.

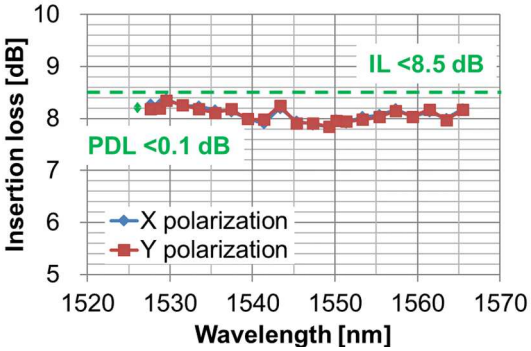

Fig. 4: Insertion loss per polarization over C-band.

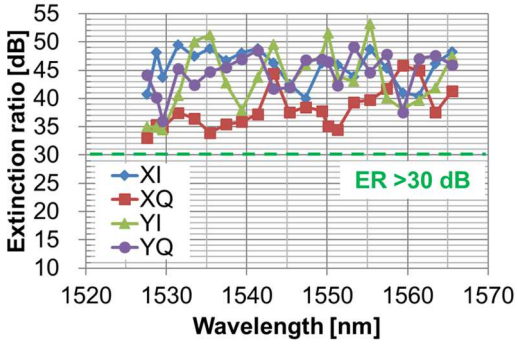

Fig. 5: Extinction ratio over C-band of the child Mach-Zehnder interferometer.

Figure 6 shows the power dissipation of the HB-CDM. The TEC was set to 50°C in the case temperature range of 0 to 75°C. The total power dissipation of the HB-CDM included the power of the driver IC, the TEC, and the modulator (heater and bias). The power dissipation was less than 5 W at these case temperatures. The breakdown of the power dissipation at 75°C is 3.25 W for the driver, 1.16 W for the TEC, and 0.49 W for the modulator.

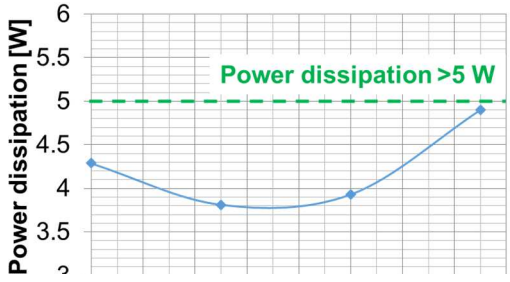

Fig. 6: Power dissipation of the HB-CDM.

Finally, we examined back-to-back DP-IQ modulated signals using the experimental setup shown in Fig. 7. The wavelength and power of the optical input were 1550 nm and +16 dBm, respectively. We used the arbitrary waveform generator (AWG, Keysight M8199A) as the RF signal source. An optical modulation analyser (OMA, Keysight N4391B) was used at the receiver end. Figure 8 shows a back-to-back constellation diagram of dual polarization 128-Gbaud 16-QAM. We confirmed a very clear constellation with a bit-error rate less than 2.0 × 10^{-2}.

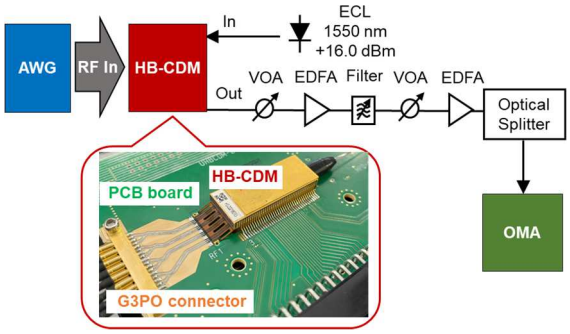

Fig. 7: Back-to-back experimental setup.

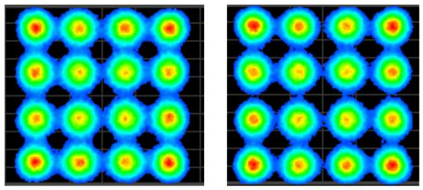

Fig. 8: 128-Gbaud DP-16-QAM back-to-back constellation diagram.

Conclusions

We developed a class-80 HB-CDM with an FPC RF interface. The HB-CDM has sufficient bandwidth (>80 GHz) and optical characteristics (IL<8.5 dB per polarization, PDL<0.1, ER>30 dB) for 128-Gbaud and higher transmission. Although we have confirmed operation up to 128 Gbaud, we believe that operation beyond 150 Gbaud is achievable because the EO bandwidth is over 80 GHz.

References

[1] K. Kikuchi, "Fundamentals of Coherent Optical Fiber Communications," *Journal of Lightwave Technology, vol.* 34, no. 1, pp. 157-179, Jan., 2016, DOI: 10.1109/JLT.2015.2463719.

[2] K. Roberts, Q. Zhuge, I. Monga, S. Gareau, and C. Laperle, "Beyond 100 Gb/s: Capacity, Flexibility, and Network Optimization," *Journal of Optical Communications and Networks*, vol. 9, no. 4, C12-C24, Apr. 2017, DOI: 10.1364/JOCN.9.000C12.

[3] J. Ozaki, Y. Ogiso, T. Jyo, Y. Hashizume, S. Kanazawa, Y. Ueda, M. Nagatani, H. Yamazaki, H. Tanobe, M, Ishikawa, "500-Gb/s/λ Operation of Ultra-Low Power and Low-Temperature-Dependence InP-Based High-Bandwidth Coherent Driver Modulator," *Journal of Lightwave Technology*, vol. 38, no. 18, pp. 5086-5091, Sept., 2020, DOI: 10.1109/JLT.2020.2998466.

[4] Implementation Agreement for the High Bandwidth Coherent Driver Modulator (HB-CDM), IA # OIF-HB-CDM-02.0, July, 2021, https://www.oiforum.com/wp-content/uploads/OIF-HB-CDM-02.0.pdf

[5] H. Yagi, T. Kaneko, N. Kono, Y. Yoneda, K. Uesaka, M. Ekawa, M. Takechi, and H. Shoji, "InP-based monolithically integrated photonics devices for digital coherent transmission," *IEEE Journal of Selected Topics in Quantum Electronics*, vol. 24, no. 1, pp. 1-11, Jan.-Feb. 2018, Art no. 6100411, DOI: 10.1109/JSTQE.2017.2725445.

[6] Implementation Agreement for Micro Integrated Coherent Receivers, IA # OIF-DPC-MRX-02.0, June, 2017, https://www.oiforum.com/wp-content/uploads/2019/01/OIF-DPC-MRX-02.0.pdf

[7] Y. -W. Chen, K. Kuzminm, R. Zhang, M. Poirier, T. Tomimoto, G. Zarris, R. Moore, C. Chen, W. Wu, J. Huang, M. Boudeau, H. Xu, and W. I. Way, "InP CDM and ICR Enabled 128Gbaud/ DP-16QAM-PS and 120Gbaud/DP-QPSK Long-Haul Transmission," *IEEE Photonics Technology Letters*, vol. 34, no. 9, pp. 471-474, May, 2022, DOI: 10.1109/LPT.2022.3165484.

[8] M. Xu, Y. Zhu, F. Pittalà, J. Tang, M. He, W. C. Ng, J. Wang, Z. Ruan, X. Tang, M. Kuschnerov, L. Liu, S. Yu, B. Zheng, and X. Cai, "Dual-polarization thin-film lithium niobate in-phase quadrature modulators for terabit-per-second transmission," *Optica* 9, 61-62, 2022, DOI: 10.1364/OPTICA.449691.

[9] S. Makino, S. Takeuchi, S. Maruyama, M. Doi, Y. Ohmori and Y. Kubota, "Demonstration of thin-film lithium niobate high-bandwidth coherent driver modulator," in *Procedings 2022 Optical Fiber Communications Conference and Exhibition (OFC)*, 2022, pp. 1-3, https://ieeexplore.ieee.org/document/9748709

[10] M. Zhang, C. Wang, P. Kharel, D. Zhu, and M. Lončar, "Integrated lithium niobate electro-optic modulators: when performance meets scalability," *Optica* 8, 652-667, 2021, DOI: 10.1364/OPTICA.415762.

[11] J. Ozaki, H. Tanobe, M. Ishikawa, "Crosstalk reduction between RF input channels of coherent-driver-modulator package by introducing enhanced ground lead structure," *Electronics Letters*, vol. 56, no. 17, pp. 893–1895, 2020, DOI: 10.1049/el.2020.1318.

[12] Y. Ogiso, J. Ozaki, Y. Ueda, H. Wakita, M. Nagatani, H. Yamazaki, M. Nakamura, T. Kobayashi, S. Kanazawa, Y. Hashizume, H. Tanobe, N. Nunoya, M. Ida, Y. Miyamoto, and M. Ishikawa, "80-GHz Bandwidth and 1.5-V Vπ InP-Based IQ Modulator," Journal of Lightwave Technology, vol. 38, no. 2, pp. 249-255, Jan. 2020, DOI: 10.1109/JLT.2019.2924671.